

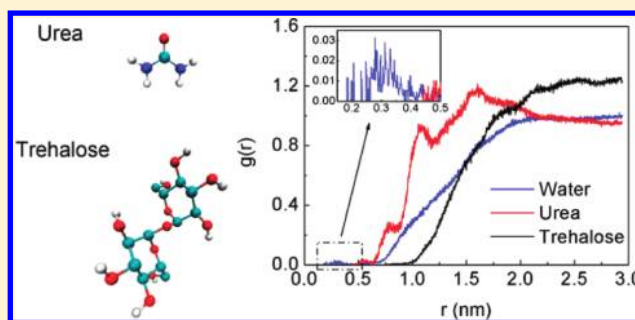
## Molecular Insight into the Counteraction of Trehalose on Urea-Induced Protein Denaturation Using Molecular Dynamics Simulation

Na Zhang, Fu-Feng Liu,\* Xiao-Yan Dong, and Yan Sun\*

Department of Biochemical Engineering and Key Laboratory of Systems Bioengineering of the Ministry of Education, School of Chemical Engineering and Technology, Tianjin University, Tianjin 300072, China

## S Supporting Information

**ABSTRACT:** Considerable experimental evidence indicates that trehalose can counteract the denaturing effects of urea on proteins. However, its molecular mechanism remains unknown due to the limitations of current experimental techniques. Herein, molecular dynamics simulations were performed to investigate the counteracting effects of trehalose against urea-induced denaturation of chymotrypsin inhibitor 2. The simulations indicate that the protein unfolds in 8 mol/L urea, but at the same condition the protein retains its native structure in the ternary solution of 8 mol/L urea and 1 mol/L trehalose. It is confirmed that the preferential exclusion of trehalose from the protein surface is the origin of its counteracting effects. It is found that trehalose binds urea via hydrogen bonds, so urea molecules are also expelled from the protein surface along with the preferential exclusion of trehalose. The exclusion of urea from the protein surface leads to the alleviation of the Lennard-Jones interactions between urea and the hydrophobic side chains of the protein in the ternary solution. In contrast, the electrostatic interactions between urea and the protein change little in the presence of trehalose because the decrease in the electrostatic interactions between urea and the protein backbone is canceled by the increase in the electrostatic interactions between urea and the charged side chains of the protein. The results have provided molecular explanations for the counteraction of urea-induced protein denaturation by trehalose.



## 1. INTRODUCTION

Osmolytes are small organic molecules that have significant effects on protein stability, structure, and function. They include amino acids and derivatives, methylamines, polyols, and urea.<sup>1,2</sup> Urea is a commonly used protein denaturant in *in vitro* unfolding/refolding experiments. In nature, some organisms or living cells are exposed to a high concentration of urea.<sup>3</sup> In order to counteract the denaturing effects of urea on proteins *in vivo*, organisms or cells utilize the other protective osmolytes,<sup>4</sup> such as methylamines (e.g., TMAO,<sup>5</sup> betaine<sup>6</sup>) and polyols, which can stabilize protein structure and maintain its activity in the presence of urea. Among the polyols, trehalose has received special attention because it has been found to be particularly efficient in protecting the function and structure of proteins against the chemical denaturation of the denaturants, such as guanidine hydrochloride<sup>7–10</sup> and urea.<sup>11</sup> For example, Kumar et al.<sup>12</sup> revealed that trehalose strongly offset the denaturing effects of urea on  $\alpha$ -chymotrypsin using differential scanning calorimeter techniques. However, the molecular mechanism for the counteracting effects of trehalose on urea-induced protein denaturation is still unknown.

Investigating the molecular mechanism of the inhibiting effects of trehalose on the protein denaturation by urea presents a major challenge, as it may lead to novel approaches in the rational design of effective protein stabilizers. However, it

seems unlikely that experimental approaches can provide the molecular details of how trehalose inhibits urea-induced protein denaturation. In recent years, many molecular dynamics (MD) simulations have been performed to study the stabilizing effects of trehalose on protein conformation.<sup>13–17</sup> For example, it was found that trehalose was preferentially excluded from the protein domain and stabilized the protein.<sup>18–20</sup> Besides, MD simulations were also used to investigate the protein denaturation by urea.<sup>21</sup> Despite many researches in the field, there is no universal molecular mechanism that can explain how urea denatures proteins. Up to now, several mechanisms have been proposed. For example, urea denatures proteins by directly binding to the protein (direct mechanism)<sup>22,23</sup> or by indirectly altering the solvent environment (indirect mechanism)<sup>24,25</sup> or even via both direct and indirect mechanisms.<sup>26,27</sup> Nevertheless, there were no systemic MD simulations on the molecular mechanism for the protection of trehalose against urea-induced protein denaturation, so we herein employ MD simulations to address this issue.

Chymotrypsin inhibitor 2 (CI2) was chosen for this study since it has been extensively used in both theoretical and

Received: January 6, 2012

Revised: May 12, 2012

Published: May 18, 2012

Table 1. Summary of Simulation Systems

no. of urea molecules	no. of trehalose molecules	no. of water molecules	urea concentration (mol/L)	trehalose concentration (mol/L)	simulation time (ns) <sup>a</sup>
0	0	6796	0	0	100 (2)
1124	0	4127	8	0	100 (2)
1058	140	2064	8	1	100 (2)

<sup>a</sup>The number of repetitive simulation runs is given in parentheses.

experimental studies with regard to protein folding/unfolding.<sup>28,29</sup> Due to the high computational demand of MD simulations, high concentrations of urea or high temperatures were often used to enhance the rate of protein unfolding.<sup>30</sup> Thus, the urea-induced denaturation of CI2 was performed in 8 mol/L urea at 333 K, which is often used in previous MD simulations.<sup>26,31,32</sup> Under these circumstances, only 1 mol/L trehalose can be added into the simulation box because of its large volume. Therefore, the concentration ratio of trehalose and urea in our MD simulations was 1:8, which is inconsistent with that of the corresponding experimental study.<sup>12</sup> The discrepancy is caused by the limitations of MD simulations, which has been proven in previous studies. For example, the interactions between amyloid peptides and inhibitors, such as phenol red,<sup>33</sup> Congo red,<sup>34</sup> thioflavin T,<sup>35</sup> trehalose,<sup>20</sup> and (–)-epigallocatechin-3-gallate,<sup>36</sup> have been widely studied using MD simulations, in which the molar ratio of amyloid  $\beta$ -peptide and its inhibitors did not accord with that of the corresponding experiments either. However, the simulation results were in good agreement with those of the experiments. Therefore, we expect that the inhibition mechanism observed in the present system is reasonable. In addition, the MD simulations of the protein in water and 8 mol/L urea at 333 K were performed for comparison. First, the properties of the protein in the ternary system of 8 mol/L urea and 1 mol/L trehalose were investigated to compare with the other two control simulations (i.e., water and 8 mol/L urea). Thereafter, the preferential exclusion effects of solvent were analyzed. Finally, the influence of trehalose on the direct interactions between urea and the protein was discussed in detail.

## 2. METHODS

**2.1. Simulation Systems.** The crystal structure of the CI2 available in Protein Data Bank (PDB) (PDB code: 1YPC)<sup>37</sup> was used as the initial structure for all MD simulations. The missing atoms of the side chain of Met40 were added using the CHARMM-GUI (<http://www.charmm-gui.org>).<sup>38</sup> The simple point charge (SPC) model<sup>39</sup> was used for water. The urea model was derived from the amide of the Asn and Gln side chains based on the GROMOS96 43a1 force field.<sup>40</sup> The initial structure of trehalose was extracted from PDB (PDB code: 2CY6).<sup>41</sup> The topology of trehalose was generated by the GlycoBioChem PRODRG2 server (<http://davapc1.bioch.dundee.ac.uk/prodr2/>).<sup>42</sup> Atomic charge and charge groups were all defined based on the existing GROMOS96 force field parameter set.

The ternary system of 8 mol/L urea and 1 mol/L trehalose was constructed as follows. First, CI2 was placed in the center of a cubic box with periodic boundary conditions. The dimension of the cubic box was set to about 6 nm such that a minimum distance between any protein atoms and the box edge is more than 1 nm. Then, trehalose molecules nonoverlapping with either the protein or trehalose were randomly added in the simulation box. Thereafter, the system

was immersed in a pre-equilibrated box of 8 mol/L urea to construct a ternary system of 8 mol/L urea and 1 mol/L trehalose. Finally, the box was filled with water molecules which were randomly added into the box with no overlap between water and the other molecules. The MD simulations of CI2 in water and 8 mol/L urea were also performed for comparison; the systems were constructed in a similar way. Finally two chloride ions were added by replacing the corresponding number of water molecules to yield a neutral condition. Table 1 summarizes the important data for the simulation systems.

After 5000 steps of steepest descent energy minimization, the system was equilibrated for 500 ps with position restraints on the protein heavy atoms. The MD simulations were then performed for 100 ns. To make certain that the effect of trehalose on the urea-induced protein denaturation is the intrinsic character of trehalose rather than the stochastic output of MD simulations, two MD simulations of 100 ns were conducted for each system under different initial conditions by assigning different initial velocities on each atom of the simulation systems (Table 1).

**2.2. Molecular Dynamics Simulations.** All MD simulations were performed using the GROMACS 4.0.5 package<sup>43</sup> with GROMOS96 43a1 force field.<sup>40</sup> A cutoff of 0.9 nm was used for Lennard-Jones interactions. Particle Mesh Ewald summation (PME)<sup>44,45</sup> was used to calculate electrostatic interactions with a grid-spacing of 0.12 nm, an interpolation order of 4, and a cutoff of 0.9 nm for short-range Coulomb interactions. All simulations were performed under the isothermal–isobaric (NPT) ensemble. Temperature (333 K) and pressure (1 atm) were controlled by the v-rescale thermostat<sup>46</sup> and Berendsen barostat,<sup>47</sup> respectively. An integration time step of 2 fs was used together with the LINCS constraint solver<sup>48</sup> for all covalent bonds. Structures were saved every 2 ps for analysis, resulting in 50 000 conformations for each 100-ns simulation. MD simulations were run on a 64-CPU Dawning A620r-F server (Dawning, Tianjin, China).

**2.3. Analysis.** The simulation trajectories were analyzed using several auxiliary programs provided with the GROMACS 4.0.5 package. The *g\_rms* program was used to compute the root-mean-square deviation of  $C\alpha$  ( $C\alpha$  rmsd) of the protein. The interaction energies between urea and the protein were analyzed using the “rerun” option of the *mdrun* program in a similar way to Lindgren et al.<sup>49</sup> Then, the *g\_energy* program was used to calculate the intermolecular electrostatic and Lennard-Jones energies between urea and the protein. It is noted that the total electrostatic energy between urea and the protein includes both the short-range and long-range parts. The radial distribution functions (RDFs) between particles were calculated using the *g\_rdf* program. It is noted that the last 10-ns trajectories were used to calculate these RDFs. In addition, secondary structure of the protein was classified using DSSP<sup>50</sup> and the snapshots of the protein structures were plotted using the visual molecular dynamics (VMD) software<sup>51</sup> (<http://www>).

ks.uiuc.edu/Research/vmd/). The number of hydrogen bonds was calculated using *g\_hbond* with a cutoff radius of 0.35 nm between donor and acceptor and a cutoff angle (acceptor–donor–hydrogen) of 30° as geometric criteria for the existence of a hydrogen bond. Except for the secondary structure of the protein, each value is the average over two MD simulations.

In order to characterize the solvent composition at the protein/solvent interface, the relative local distribution of water, urea and trehalose molecules around CI2 was characterized in a similar way to Lerbret et al.<sup>18,19</sup> The time-averaged normalized ratios of water oxygen, urea carbon and trehalose hydroxyl oxygen,  $g_{OW}$ ,  $g_{CU}$  and  $g_{OT}$  in different solutions were defined as follows:

$$g_{OW}(r) = \frac{n_{OW}(r)/[n_{OW}(r) + n_{CU}(r) + n_{OT}(r)]}{N_{OW}/[N_{OW} + N_{CU} + N_{OT}]} \quad (1)$$

$$g_{CU}(r) = \frac{n_{CU}(r)/[n_{OW}(r) + n_{CU}(r) + n_{OT}(r)]}{N_{CU}/[N_{OW} + N_{CU} + N_{OT}]} \quad (2)$$

$$g_{OT}(r) = \frac{n_{OT}(r)/[n_{OW}(r) + n_{CU}(r) + n_{OT}(r)]}{N_{OT}/[N_{OW} + N_{CU} + N_{OT}]} \quad (3)$$

where  $n_{OW}(r)$ ,  $n_{CU}(r)$ , and  $n_{OT}(r)$  are the local numbers of water oxygen atoms, urea carbon atoms, and trehalose hydroxyl oxygen atoms, respectively, located at a minimum distance ( $r$ ) from the center of mass (COM) of the protein and  $N_{OW}$ ,  $N_{CU}$ , and  $N_{OT}$  denote the total numbers of water oxygen atoms, urea carbon atoms, and trehalose hydroxyl oxygen atoms in the simulation box, respectively.

### 3. RESULTS AND DISCUSSION

**3.1. Protein Properties in Different Solvent Environments.** To understand whether trehalose can protect against the denaturing effects of urea on the protein, the values of  $\alpha$  rmsd in water, 8 mol/L urea, and the ternary solution of 8 mol/L urea and 1 mol/L trehalose were calculated and displayed as a function of time in Figure 1a. In water, the values of  $\alpha$  rmsd approach stable after 5 ns, implying that the protein maintains its native structure. However, the  $\alpha$  rmsd values in 8 mol/L urea increase greatly after about 50 ns. It means that CI2 is denatured in 8 mol/L urea, which is in agreement with previous experimental<sup>52</sup> and theoretical<sup>26,31</sup> results. In fact, the values of  $\alpha$  rmsd in the ternary solution of 8 mol/L urea and 1 mol/L trehalose are most similar to those in water (Figure 1a). It indicates that trehalose can efficiently counteract the urea-induced protein denaturation. Figure 1b shows the CI2 crystal and the final snapshots in 100-ns MD simulations in different solutions. The structures of CI2 in water and the ternary solution are similar to the crystal structure. In 8 mol/L urea, however, the C- and N- terminals slide aside and the protein is extended, resulting in the exposure of the hydrophobic core to the solvent. Obviously, the  $\beta$ -strand at the C-terminal has changed into a coil structure. It is further confirmed that the protein unfolds in 8 mol/L urea while 1 mol/L trehalose can inhibit the denaturing effects of urea on the protein.

To probe the conformational transition of the protein in different solutions, the secondary structure was determined by DSSP<sup>50</sup> (Figure 2). In water, there is no significant conformational transition, especially for the four typical secondary-structures (i.e., one  $\alpha$ -helix and three  $\beta$ -strands; Figure 2a). In 8 mol/L urea, however, the  $\beta$ -strand at the C-terminal completely disappears after 90 ns and the content of the other two  $\beta$ -

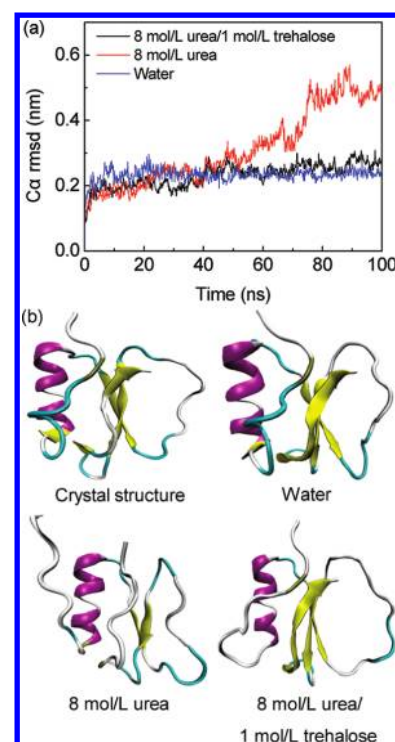


**Figure 1.** (a) Root mean square deviation (rmsd) for  $\alpha$  atoms from the crystal structure of CI2 as a function of simulation time in different solutions. (b) CI2 crystal structure and the final structures in 100-ns MD simulations in different solutions. The protein is shown by a NewCartoon model. The secondary structures of the protein are characterized by different colors. Purple,  $\alpha$ -helix; yellow,  $\beta$ -strand; white, coil; green, turn.

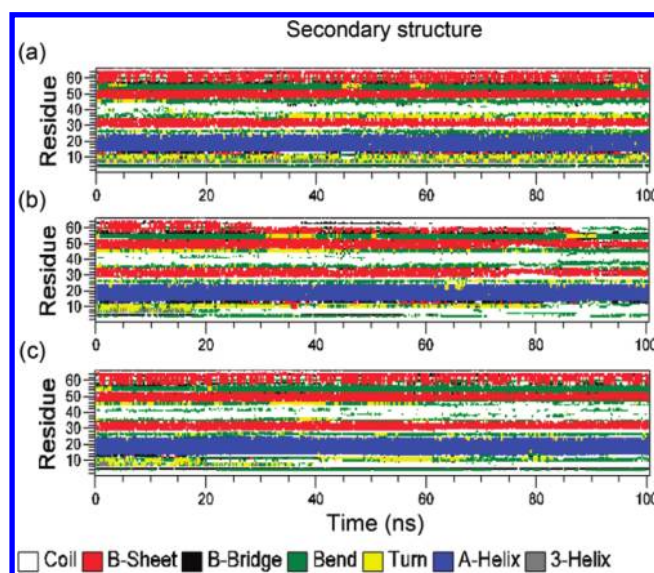


**Figure 2.** Secondary structures as a function of simulation time for CI2 in different solutions: (a) water, (b) 8 mol/L urea, and (c) a ternary solution of 8 mol/L urea and 1 mol/L trehalose. The vertical coordinate represents the residue number, and the secondary structure is color-coded as given in the bottom of the figure.

strands partially decreases with increasing simulation time, although the  $\alpha$ -helix keeps well during the whole simulation (Figure 2b). When trehalose is introduced, all of the native secondary structure elements of the protein are well maintained (Figure 2c). That is, 1 mol/L trehalose can offset the



denaturing effect of urea on the protein and make the protein maintain its native conformation.

**3.2. Preferential Exclusion Effects.** Preferential exclusion is commonly considered as a reason of the stabilizing effects of protective osmolytes such as trehalose on proteins.<sup>53</sup> The mechanism indicates that trehalose molecules are excluded from the protein surface and water molecules in the hydration shell around the protein increase, thus inducing thermodynamic stabilization of proteins. In order to investigate the preferential interactions of solvent with the protein in different solutions, the distribution of solvent molecules at the protein surface was calculated using RDFs between solvent molecules and the protein (Figures 3, S1 and S2). The COM of the protein, water

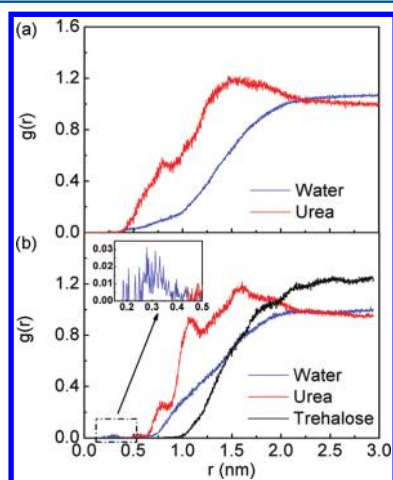


**Figure 3.** Radial distribution functions for water oxygen, urea carbon, and trehalose hydroxyl oxygen around the center of mass (COM) of the protein as a function of the distance  $r$  from the COM of the protein in 8 mol/L urea (a) and a ternary solution of 8 mol/L urea and 1 mol/L trehalose (b) over the last 10 ns of the simulation.

oxygen, urea carbon, and trehalose hydroxyl oxygen were used in RDFs calculation, which are often utilized in some previous MD simulations.<sup>54–56</sup> In 8 mol/L urea (Figures 3a and S1), the urea density in the approximate range 0.25–2.2 nm from the COM of the protein is larger than that of water in the corresponding range, meaning that a large number of urea molecules distribute around the protein and water molecules are expelled from the protein surface. It can be indicated that there are strong direct interactions between urea and the protein, which induce the denaturation of CI2. The phenomenon is in good agreement with some previous simulation results.<sup>23,49</sup> However, in the ternary solution of 8 mol/L urea and 1 mol/L trehalose (Figures 3b and S2), there is an increase in the water density within a distance of about 0.35 nm from the COM of the protein. However, the urea density decreases significantly in comparison with the corresponding values in 8 mol/L urea. That is, urea molecules are excluded from the protein surface and a few water molecules exist within a distance of about 0.45 nm from the COM of the protein (inset of Figures 3b and S2) in the ternary solution. In addition, the trehalose molecules only distribute in the approximate range of larger than 1.0 nm from the COM of the protein, implying that trehalose molecules are preferentially excluded from the domain of the protein, which has been proven to be the main reason that trehalose could stabilize proteins.<sup>18–20</sup> It can be seen from Table 2 that about two hydrogen bonds are formed between trehalose and the protein, which are far fewer

**Table 2.** Mean Number of Hydrogen Bonds between Different Molecules in Different Solutions<sup>a</sup>

system	protein–urea	protein–trehalose	trehalose–urea
8 mol/L urea	109 ± 9		
8 mol/L urea/1 mol/L trehalose	104 ± 9	2 ± 1	56 ± 6

<sup>a</sup>All values are averaged over the last 10 ns of the two simulations.

than those trehalose molecules could form with the protein. It further indicates the preferential exclusion of trehalose from the protein surface.

To further quantify the preferential interactions between solvent components and the protein, the relative local distribution of water, urea and trehalose molecules (eqs 1–3) around CI2 was characterized in a similar way to Lerbret et al.<sup>18,19</sup> Equations 1–3 indicate that the ratio ( $g_{OW}$ ,  $g_{Cu}$  or  $g_{Ot}$ ) is greater than 1 in the proximity of the protein if the solvent preferentially interacts with the protein. Conversely, the solvent is preferentially excluded from the protein surface if the ratio is lower than 1. Data were plotted between 0.3 and 3.0 nm from the COM of the protein.

Figure 4 shows the normalized fraction of water oxygen ( $g_{OW}$ ), urea carbon ( $g_{Cu}$ ), and trehalose hydroxyl oxygen ( $g_{Ot}$ )

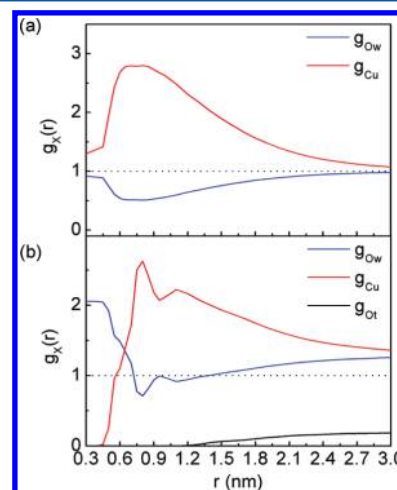


**Figure 4.** Normalized fraction of water oxygen ( $g_{OW}$ ), urea carbon ( $g_{Cu}$ ), and trehalose hydroxyl oxygen ( $g_{Ot}$ ) as a function of the minimum distance  $r$  from the center of mass (COM) of the protein in 8 mol/L urea (a) and a ternary solution of 8 mol/L urea and 1 mol/L trehalose (b) over the last 10 ns of the simulation.

as a function of the minimum distance from the COM of CI2 in different solutions. In 8 mol/L urea (Figure 4a),  $g_{Cu}$  is greater than 1, whereas  $g_{OW}$  is less than 1 through all the distance from the COM of the protein, implying that urea molecules expel water from the surface of CI2, interact directly with the protein, and denature the protein. However, in the ternary solution of 8 mol/L urea and 1 mol/L trehalose (Figure 4b),  $g_{Cu}$  is lower than 1, whereas  $g_{OW}$  is greater than 1 within a distance of about 0.6 nm from the COM of CI2. It is further confirmed that urea molecules are expelled from the protein surface and the protein is preferentially hydrated. Thus, the direct interactions between urea and the protein are greatly alleviated by trehalose. Besides,  $g_{Ot}$  is lower than 1 in the approximate range of larger than 1.2 nm from the COM of CI2, further indicating that trehalose molecules are preferentially excluded from the surface of the

protein. Therefore, it can be concluded that the addition of trehalose leads to the exclusion of urea from the protein surface.

As mentioned above, urea is excluded from the protein surface in the ternary solution. However, the reason for the exclusion of urea from the protein surface is still unclear. It is known that trehalose includes eight hydroxyl groups and it can form multihydrogen bonds. Meanwhile, urea can provide hydrogen atoms through its amino groups and accept hydrogen atoms through its carbonyl group. So, one urea can form two or more hydrogen bonds.<sup>57</sup> This suggests that trehalose could interact with the amino and/or carbonyl groups of urea by hydrogen bonds via its hydroxyl groups. It was calculated that about 56 hydrogen bonds are formed between trehalose and urea in the ternary solution (Table 2). That is, trehalose binds urea via hydrogen bonds, so urea molecules are also expelled from the protein surface along with the preferential exclusion of trehalose in the ternary solution of 8 mol/L urea and 1 mol/L trehalose. This phenomenon is similar to the behavior of TMAO<sup>31,58</sup> in which the attracting hydrogen bonds between TMAO and urea decrease the concentration of urea at the protein surface, thus counteracting the urea-induced protein denaturation. Therefore, the preferential exclusion of trehalose combined with the hydrogen bonds between trehalose and urea is the origin of its inhibiting effects on the urea-induced protein denaturation.

**3.3. Direct Interactions between Urea and the Protein Are Alleviated by Trehalose.** According to the above results, it is known that urea is excluded from the protein surface in the presence of trehalose and thus decreases the direct interactions between urea and the protein. To probe the direct interactions between urea and the protein affected by trehalose, the intermolecular electrostatic and Lennard-Jones energies between urea and the protein were calculated during the whole simulation in different solutions (Figure 5). It can be

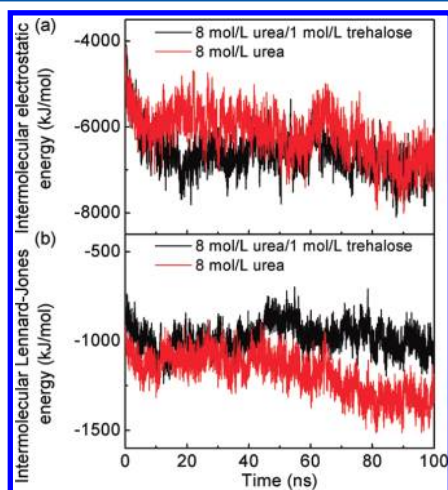


**Figure 5.** Intermolecular electrostatic (a) and Lennard-Jones (b) energies between urea and the protein as a function of simulation time in different solutions.

seen from Figure 5a that the electrostatic energy between urea and the protein remains almost unchanged when 1 mol/L trehalose is added into 8 mol/L urea solution. However, there is a significant decrease from about  $-1000$  to  $-1300$  kJ/mol in the Lennard-Jones energy between urea and the protein after 80 ns in 8 mol/L urea solution with respect to the ternary

system (Figure 5b). It indicates that the Lennard-Jones interactions between urea and the protein are greatly alleviated by trehalose.

Within the direct interaction mechanism of urea-induced protein denaturation, there is a controversy over which interactions (electrostatic or van der Waals) are dominant. The “direct electrostatic mechanism”<sup>59–61</sup> implies that urea directly interacts with the protein backbone and charged and polar side chains via electrostatic interactions. In contrast, the “direct van der Waals mechanism” considers that urea denatures proteins predominantly through its van der Waals interactions.<sup>23,32,62</sup> It can be inferred from the above results that the Lennard-Jones interactions rather than the electrostatic interactions between urea and the protein are the driving force for urea-induced protein denaturation. These observations are also consistent with some previous results.<sup>23,62</sup> For example, Lindgren et al.<sup>49</sup> have found that the addition of urea increased the Lennard-Jones interactions between solvent and protein by a large amount but it did not affect their electrostatic interactions. Besides, Kokubo et al.<sup>63</sup> also found that the denaturation of a decaalanine peptide induced by urea was dominated by the van der Waals interactions.

In order to further investigate the details of the interactions between urea and the protein, the protein atoms are classified into the backbone, the charged side chains and the hydrophobic side chains. As mentioned above, urea could form multihydrogen bonds.<sup>57</sup> According to Jeffrey’s classification, the nature of hydrogen bonds is mainly electrostatic interaction.<sup>64</sup> In addition, urea does not include net charge. Therefore, the electrostatic interactions between urea and the protein can be represented by their hydrogen bond interactions.<sup>60</sup> Herein, a number of RDFs of urea atoms (hydrogen and oxygen) with those atoms of the backbone and the charged side chains of the protein were used to give an insight of the donor/acceptor interactions in different solutions.

The hydrogen bond interactions of urea with the backbone of CI2 can be obtained from the RDFs between hydrogen atoms in urea ( $H_U$ ) and backbone carbonyl oxygen atoms ( $O_B$ ) of the protein (Figure 6a) and between oxygen atoms in urea ( $O_U$ ) and backbone amide hydrogen atoms ( $H_B$ ) of the protein (Figure 6b), respectively. From Figure 6a, the  $O_B-H_U$  RDF shows two distinct peaks around 0.21 and 0.35 nm. The peak at 0.21 nm corresponds to the hydrogen bonds formed between two amino groups of urea and the carbonyl group of the

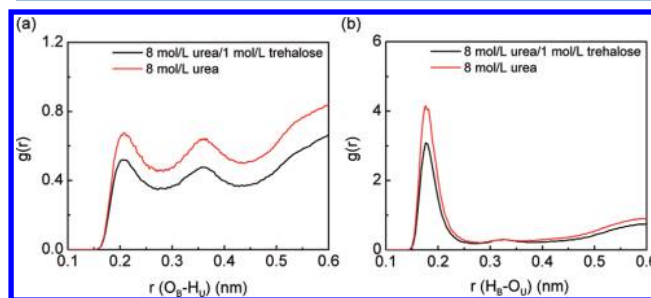


**Figure 6.** Radial distribution functions between urea and the backbone of CI2 in 8 mol/L urea and a ternary solution of 8 mol/L urea and 1 mol/L trehalose over the last 10 ns of the simulation. (a) Radial distribution functions between hydrogen atoms in urea ( $H_U$ ) and oxygen atoms of backbone carbonyl groups of CI2 ( $O_B$ ). (b) Radial distribution functions between oxygen atoms in urea ( $O_U$ ) and hydrogen atoms of backbone amino groups of CI2 ( $H_B$ ).

protein backbone, and the peak at 0.35 nm implies that other interactions exist between these groups. Meanwhile, the  $H_B-O_U$  RDF shows a peak at about 0.18 nm (Figure 6b), implying that hydrogen bonds are also formed between the carbonyl group of urea and the amino group of the protein backbone. It is noted that all of the peaks in 8 mol/L urea are larger than those in the ternary solution, suggesting that the hydrogen bond interactions between urea and the protein backbone are weakened by trehalose. Figure 7a shows the RDFs between hydrogen

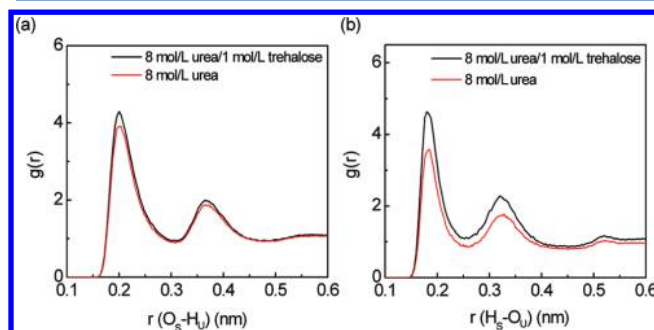


**Figure 7.** Radial distribution functions between urea and the charged side chains of CI2 in 8 mol/L urea and a ternary solution of 8 mol/L urea and 1 mol/L trehalose over the last 10 ns of the simulation. (a) Radial distribution functions between hydrogen atoms in urea ( $H_U$ ) and oxygen atoms of the negatively charged side chains of CI2 ( $O_S$ ). (b) Radial distribution functions between oxygen atoms in urea ( $O_U$ ) and hydrogen atoms of the positively charged side chains of CI2 ( $H_S$ ).

atoms ( $H_U$ ) in urea and oxygen atoms of the negatively charged side chains ( $O_S$ ), exhibiting two peaks around 0.20 and 0.35 nm. The RDFs between oxygen atoms in urea ( $O_U$ ) and hydrogen atoms of the positively charged side chains ( $H_S$ ) with two peaks around 0.18 and 0.32 nm are shown in Figure 7b. The peaks around 0.20 nm (Figure 7a) and 0.18 nm (Figure 7b) indicate that urea hydrogen and oxygen form hydrogen bonds with oxygen of the negatively charged side chains and hydrogen of the positively charged side chains, respectively. Besides, the additional peaks approximately at 0.35 nm (Figure 7a) and 0.32 nm (Figure 7b) correspond to other interactions between urea and the charged side chains of the protein. It is evident that all of the peaks in 8 mol/L urea are lower than those in the ternary solution, indicating that the hydrogen bond interactions between urea and the charged side chains of the protein increase in the presence of trehalose. The increase in the hydrogen bond interactions between urea and the charged side chains of the protein is canceled by the decrease in the hydrogen bond interactions between urea and the protein backbone. Besides, it can be seen from Table 2 that there is little change in the number of hydrogen bonds between urea and the protein in the presence of trehalose compared with that in 8 mol/L urea ( $109 \pm 9$  hydrogen bonds on average in 8 mol/L urea and  $104 \pm 9$  hydrogen bonds on average in the ternary solution). In other words, the electrostatic interactions between urea and the protein contribute little to the urea-induced protein denaturation, as also shown in Figure 5a.

To further investigate the effect of trehalose on the Lennard-Jones interactions between urea and the hydrophobic side chains of the protein, the RDFs between carbon atoms in urea ( $C_U$ ) and  $C_\beta$  atoms of the hydrophobic residues ( $C_\beta$ ) were calculated (Figure 8) in a similar way to previous research.<sup>22,23,27</sup> The plot shows a peak at about 0.45 nm. The peak corresponds to the Lennard-Jones interactions between

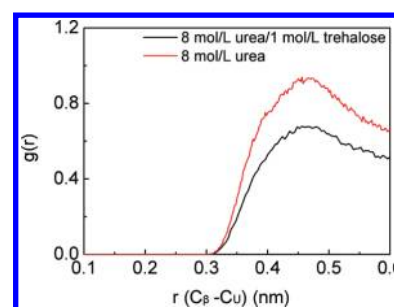


**Figure 8.** Radial distribution functions between carbon atoms in urea ( $C_U$ ) and  $C_\beta$  atoms of the hydrophobic residues of CI2 ( $C_\beta$ ) in 8 mol/L urea and a ternary solution of 8 mol/L urea and 1 mol/L trehalose over the last 10 ns of the simulation.

urea and the hydrophobic side chains of the protein. It is found that the peak in 8 mol/L urea is much higher than that in the ternary solution. It means that the Lennard-Jones interactions between urea and the hydrophobic side chains of the protein are greatly alleviated by trehalose.

It can thus be concluded that the addition of trehalose greatly reduces the Lennard-Jones interactions between urea and the hydrophobic side chains of the protein. However, the electrostatic interactions (i.e., hydrogen bond interactions) between urea and the protein change little in the presence of trehalose. It is further confirmed that the electrostatic interactions between urea and the protein are not the dominating force for the urea-induced protein denaturation. The results are similar to the previous conclusions. For example, Gao et al.<sup>65</sup> found that there were more urea molecules accumulated on the surface of the noncharged residues rather than the charged ones of lysozyme in 8 mol/L urea. Besides, Wei et al.<sup>66</sup> mutated two charged lysine residues of  $\beta$ -hairpin to apolar leucine and found that the mutation enhances the accumulation of urea near the hydrophobic core and facilitates the denaturation process. Both the results mean that the interactions between urea and the charged residues of the protein have no significant effects on the protein denaturation induced by urea.

#### 4. CONCLUSIONS

All-atom MD simulations were performed to investigate the counteraction of urea-induced denaturation of CI2 by trehalose. It is found that CI2 unfolds completely in 8 mol/L urea. By introducing 1 mol/L trehalose, the native structure of the protein is well maintained. In 8 mol/L urea, a large number of urea molecules displace water at the protein surface and interact directly with the protein to denature it. On the contrary, in the ternary solution of 8 mol/L urea and 1 mol/L trehalose, trehalose binds urea via hydrogen bonds, so urea molecules are also expelled from the protein surface along with the preferential exclusion of trehalose, leading to the preferential hydration of CI2. Furthermore, the exclusion of urea evidently reduces the Lennard-Jones interactions between urea and the hydrophobic side chains of the protein so that the Lennard-Jones interactions between urea and the protein are greatly alleviated. In contrast, the electrostatic interactions (i.e., hydrogen bond interactions) between urea and the protein are almost unchanged in the ternary solution. The reason is that the decrease in the electrostatic interactions between urea and the protein backbone is canceled by the increase in the electrostatic interactions between urea and the charged side



chains of the protein. Therefore, it can be concluded that urea molecules directly denature CI2 in our simulations through the direct Lennard-Jones mechanism rather than the direct electrostatic mechanism. This work has thus elucidated the molecular mechanism of the counteraction of urea-induced protein denaturation by trehalose.

## ■ ASSOCIATED CONTENT

### ■ Supporting Information

Additional information (Figures S1 and S2) is provided. Figure S1 shows the radial distribution functions for water oxygen and urea carbon around the center of mass (COM) of the protein as a function of the distance  $r$  from the COM of the protein for the two simulations over the last 10 ns of the simulation; Figure S2 shows the radial distribution functions for water oxygen, urea carbon and trehalose hydroxyl oxygen around the center of mass (COM) of the protein as a function of the distance  $r$  from the COM of the protein for the two simulations over the last 10 ns of the simulation. This material is available free of charge via the Internet at <http://pubs.acs.org>.

## ■ AUTHOR INFORMATION

### Corresponding Author

\*(F.-F.L.) Tel: +86 22 27406590. Fax: +86 22 27406590. E-mail: [fufengliu@tju.edu.cn](mailto:fufengliu@tju.edu.cn). (Y.S.) Tel: +86 22 27404981. Fax: +86 22 27406590. E-mail: [ysun@tju.edu.cn](mailto:ysun@tju.edu.cn).

### Notes

The authors declare no competing financial interest.

## ■ ACKNOWLEDGMENTS

This work was supported by the Natural Science Foundation of China (No. 20906068), the National Basic Research Program of China (973 Program, No. 2009CB724705), and the Natural Science Foundation of Tianjin from Tianjin Municipal Science and Technology Commission (Contract No. 10JCYBJC04500).

## ■ REFERENCES

- (1) Yancey, P. H. *Am. Zool.* **2001**, *41*, 699–709.
- (2) Yancey, P. H. *J. Exp. Biol.* **2005**, *208*, 2819–2830.
- (3) Barton, K. N.; Buhr, M. M.; Ballantyne, J. S. *Am. J. Physiol.* **1999**, *276*, 397–406.
- (4) Yancey, P. H.; Somero, G. N. *Biochem. J.* **1979**, *183*, 317–323.
- (5) Kelly, R. H.; Yancey, P. H. *Biol. Bull.* **1999**, *196*, 18–25.
- (6) Yancey, P. H.; Burg, M. B. *Am. J. Physiol.* **1990**, *258*, 198–204.
- (7) Sola-Penna, M.; Meyer-Fernandes, J. R. *Z. Naturforsch. C* **1996**, *51*, 160–164.
- (8) Melo, E. P.; Faria, T. Q.; Martins, L. O.; Gonçalves, A. M.; Cabral, J. M. S. *Proteins: Struct., Funct., Bioinform.* **2001**, *42*, 542–552.
- (9) Tanaka, M.; Machida, Y.; Niu, S. Y.; Ikeda, T.; Jana, N. R.; Doi, H.; Kurosawa, M.; Nekooki, M.; Nukina, N. *Nat. Med.* **2004**, *10*, 148–154.
- (10) Saadati, Z.; Bordbar, A. K. *Protein J.* **2008**, *27*, 455–460.
- (11) Lopes, D. H. J.; Meyer-Fernandes, J. R.; Sola-Penna, M. *Z. Naturforsch. C* **1999**, *54*, 186–190.
- (12) Kumar, A.; Attri, P.; Venkatesu, P. *Int. J. Biol. Macromol.* **2010**, *47*, 540–545.
- (13) Cottone, G.; Ciccotti, G.; Cordone, L. *J. Chem. Phys.* **2002**, *117*, 9862–9866.
- (14) Cottone, G.; Giuffrida, S.; Ciccotti, G.; Cordone, L. *Proteins: Struct., Funct., Bioinform.* **2005**, *59*, 291–302.
- (15) Cottone, G. *J. Phys. Chem. B* **2007**, *111*, 3563–3569.
- (16) Liu, F. F.; Dong, X. Y.; Sun, Y. *J. Mol. Graph. Model.* **2008**, *27*, 421–429.
- (17) Liu, F. F.; Ji, L.; Zhang, L.; Dong, X. Y.; Sun, Y. *J. Chem. Phys.* **2010**, *132*, 225103.
- (18) Lerbret, A.; Bordat, P.; Affouard, F.; Hedoux, A.; Guinet, Y.; Descamps, M. *J. Phys. Chem. B* **2007**, *111*, 9410–9420.
- (19) Lerbret, A.; Affouard, F.; Bordat, P.; Wdoux, A.; Guinet, Y.; Descamps, A. *Chem. Phys.* **2008**, *345*, 267–274.
- (20) Liu, F. F.; Ji, L.; Dong, X. Y.; Sun, Y. *J. Phys. Chem. B* **2009**, *113*, 11320–11329.
- (21) Lindgren, M.; Sparrman, T.; Westlund, P.-O. *Spectrochim. Acta A* **2010**, *75*, 953–959.
- (22) Das, A.; Mukhopadhyay, C. *J. Phys. Chem. B* **2008**, *112*, 7903–7908.
- (23) Hua, L.; Zhou, R. H.; Thirumalai, D.; Berne, B. J. *Proc. Natl. Acad. Sci. U. S. A.* **2008**, *105*, 16928–16933.
- (24) Stumpe, M. C.; Grubmüller, H. *J. Phys. Chem. B* **2007**, *111*, 6220–6228.
- (25) Idrissi, A.; Gerard, M.; Damay, P.; Kiselev, M.; Puhovsky, Y.; Cinar, E.; Lagant, P.; Vergoten, G. *J. Phys. Chem. B* **2010**, *114*, 4731–4738.
- (26) Bennion, B. J.; Daggett, V. *Proc. Natl. Acad. Sci. U.S.A.* **2003**, *100*, 5142–5147.
- (27) Das, A.; Mukhopadhyay, C. *J. Phys. Chem. B* **2009**, *113*, 12816–12824.
- (28) Fersht, A. R.; Daggett, V. *Cell* **2002**, *108*, 573–582.
- (29) Lindgren, M.; Westlund, P.-O. *Biophys. Chem.* **2010**, *151*, 46–53.
- (30) Eberini, I.; Emerson, A.; Sensi, C.; Ragona, L.; Ricchiuto, P.; Pedretti, A.; Gianazza, E.; Tramontano, A. *J. Mol. Graph. Model.* **2011**, *30*, 24–30.
- (31) Bennion, B. J.; Daggett, V. *Proc. Natl. Acad. Sci. U.S.A.* **2004**, *101*, 6433–6438.
- (32) Stumpe, M. C.; Grubmüller, H. *PLoS Comput. Biol.* **2008**, *4*, e1000221.
- (33) Wu, C.; Lei, H. X.; Wang, Z. X.; Zhang, W.; Duan, Y. *Biophys. J.* **2006**, *91*, 3664–3672.
- (34) Wu, C.; Wang, Z. X.; Lei, H. X.; Zhang, W.; Duan, Y. *J. Am. Chem. Soc.* **2007**, *129*, 1225–1232.
- (35) Wu, C.; Wang, Z. X.; Lei, H. X.; Duan, Y.; Bowers, M. T.; Shea, J.-E. *J. Mol. Biol.* **2008**, *384*, 718–729.
- (36) Liu, F. F.; Dong, X. Y.; He, L. Z.; Middelberg, A. P. J.; Sun, Y. *J. Phys. Chem. B* **2011**, *115*, 11879–11887.
- (37) Harpaz, Y.; Elmasry, N.; Fersht, A. R.; Henrick, K. *Proc. Natl. Acad. Sci. U.S.A.* **1994**, *91*, 311–315.
- (38) Jo, S.; Kim, T.; Iyer, V. G.; Im, W. J. *Comput. Chem.* **2008**, *29*, 1859–1865.
- (39) Berendsen, H. J. C.; Postma, J. P. M.; van Gunsteren, W. F.; Hermans, J. *Intermolecular Forces*; Pullman, B., ed.; Reidel: Dordrecht, The Netherlands, 1981; p 331.
- (40) Van Gunsteren, W. F.; Billeter, S. R.; Eising, A. A.; Hünenberger, P. H.; Krüger, P.; Mark, A. E.; Scott, W. R. P.; Tironi, I. G. *Biomolecular Simulation: The GROMOS96 Manual and User Guide*; Zürich, Switzerland, 1996.
- (41) Delatorre, P.; Rocha, B. A. M.; Gadelha, C. A. A.; Santi-Gadelha, T.; Cajazeiras, J. B.; Souza, E. P.; Nascimento, K. S.; Freire, V. N.; Sampaio, A. H.; Azevedo, W. F.; Cavada, B. S. *J. Struct. Biol.* **2006**, *154*, 280–286.
- (42) Schüttelkopf, A. W.; van Aalten, D. M. F. *Acta Crystallogr., Sect D* **2004**, *60*, 1355–1363.
- (43) Hess, B.; Kutzner, C.; van der Spoel, D.; Lindahl, E. *J. Chem. Theory Comput.* **2008**, *4*, 435–447.
- (44) Darden, T.; York, D.; Pedersen, L. *J. Chem. Phys.* **1993**, *98*, 10089–10092.
- (45) Essmann, U.; Perera, L.; Berkowitz, M. L.; Darden, T.; Lee, H.; Pedersen, L. G. *J. Chem. Phys.* **1995**, *103*, 8577–8593.
- (46) Bussi, G.; Donadio, D.; Parrinello, M. *J. Chem. Phys.* **2007**, *126*, 014101.
- (47) Berendsen, H. J. C.; Postma, J. P. M.; van Gunsteren, W. F.; Dinola, A.; Haak, J. R. *J. Chem. Phys.* **1984**, *81*, 3684–3690.
- (48) Hess, B.; Bekker, H.; Berendsen, H. J. C.; Fraaije, J. G. E. M. *J. Comput. Chem.* **1997**, *18*, 1463–1472.

- (49) Lindgren, M.; Westlund, P.-O. *Phys. Chem. Chem. Phys.* **2010**, *12*, 9358–9366.
- (50) Kabsch, W.; Sander, C. *Biopolymers* **1983**, *22*, 2577–2637.
- (51) Humphrey, W.; Dalke, A.; Schulten, K. *J. Mol. Graph.* **1996**, *14*, 33–38.
- (52) Ortore, M. G.; Sinibaldi, R.; Spinozzi, F.; Carsughi, F.; Clemens, D.; Bonincontro, A.; Mariani, P. *J. Phys. Chem. B* **2008**, *112*, 12881–12887.
- (53) Timasheff, S. N. *Biochemistry* **2002**, *41*, 13473–13482.
- (54) Dickey, A. N.; Faller, R. *Biophys. J.* **2007**, *92*, 2366–2376.
- (55) Reddy, A. S.; Izmitli, A.; de Pablo, J. J. *J. Chem. Phys.* **2009**, *131*, 085101.
- (56) Canchi, D. R.; Paschek, D.; Garcia, A. E. *J. Am. Chem. Soc.* **2010**, *132*, 2338–2344.
- (57) Boiocchi, M.; Del Boca, L.; Gómez, D. E.; Fabbrizzi, L.; Licchelli, M.; Monzani, E. *J. Am. Chem. Soc.* **2004**, *126*, 16507–16514.
- (58) Zou, Q.; Bennion, B. J.; Daggett, V.; Murphy, K. P. *J. Am. Chem. Soc.* **2002**, *124*, 1192–1202.
- (59) Mountain, R. D.; Thirumalai, D. *J. Am. Chem. Soc.* **2003**, *125*, 1950–1957.
- (60) Tobi, D.; Elber, R.; Thirumalai, D. *Biopolymers* **2003**, *68*, 359–369.
- (61) O'Brien, E. P.; Dima, R. I.; Brooks, B.; Thirumalai, D. *J. Am. Chem. Soc.* **2007**, *129*, 7346–7353.
- (62) Zangi, R.; Zhou, R. H.; Berne, B. J. *J. Am. Chem. Soc.* **2009**, *131*, 1535–1541.
- (63) Kokubo, H.; Hu, C. Y.; Pettitt, B. M. *J. Am. Chem. Soc.* **2011**, *133*, 1849–1858.
- (64) Jeffrey, G. A. *An Introduction to Hydrogen Bonding*; Oxford University Press: New York, 1997.
- (65) Gao, M.; She, Z. S.; Zhou, R. H. *J. Phys. Chem. B* **2010**, *114*, 15687–15693.
- (66) Wei, H. Y.; Yang, L. J.; Gao, Y. Q. *J. Phys. Chem. B* **2010**, *114*, 11820–11826.